Journal of New Materials for Electrochemical Systems 15, 157-163 (2012)

Effect of WO_x Over Ni/Hydrotalcite Catalysts to Produce Hydrogen from Ethanol

J.L. Contreras[1,*], M.A. Ortiz[1], G.A. Fuentes[2], M. Ortega[3], R. Luna[1], M. Gordon[1], J. Salmones[4], B. Zeifert[4], L. Nuño[1] and T. Vázquez[1]

[1]Depto. de Energía, CBI, Universidad Autónoma Metropolitana-Azcapotzalco, Av. Sn. Pablo 180 Col. Reynosa, Azcapotzalco C.P.02200 México D.F., México.
[2]Depto. de IPH, CBI, Universidad Autónoma Metropolitana-Iztapalapa, México, D.F., México
[3]Centro de Nanotecnologia del IPN, UPALM, Zacatenco, México, D.F., México
[4]ESIQIE, Instituto Politécnico Nacional, Unidad Prof. UPALM, México, D. F., 07738, México

Received: November 27, 2011, Accepted: February 10, 2012, Available online: April 04, 2012

Abstract: *The effect of WO_x over Ni-hydrotalcite catalysts to produce H_2 by ethanol steam reforming was studied. The catalysts were characterized by N_2 physisorption (BET area), X-ray diffraction, Infrared and UV-vis spectroscopies. The W concentration ranged from 0.5 to 3 wt%. As W concentration increased, the intensity of XRD reflections of the Ni catalysts decreased. The porous structure of the materials consisted of parallel layers with a monomodal mesoporous distribution. The surface groups detected by IR were: -OH, Al-OH, Mg-OH, W=O and CO_3^{2-}. UV-vis results suggested that Ni^{2+} ions were substituted by W ions. The catalytic evaluations were made in a fixed bed reactor using a water/ethanol mol ratio of 4 at 450°C. Catalysts with low loadings of W (0.5 and 1%) showed the highest H_2 production and stability. W promoted the conversion of ethanol towards hydrogen in the case of the Ni-hydrotalcite catalysts. The reaction products were; H_2, CO_2, CH_3CHO, CH_4 and C_2H_4. The catalysts did not produce CO.*

Keywords: Hydrogen, Ni, WO_x, Hydrotalcite, Ethanol

1. INTRODUCTION

Ethanol has several advantages over fossil fuel-derived hydrocarbons as a renewable source of hydrogen. It is nearly CO_2 neutral, it is less toxic; it can be more easily stored without significant handling risk and it can be obtained in large quantities from biomass [1-2].

The catalytic ethanol steam reforming has been proposed to produce hydrogen. This reaction is endothermic and it only produces H_2 and CO_2 if the ethanol reacts in the most desirable way. However, undesirable products such as CO and CH_4 are also in general formed [1]. Other reactions may occur, such as dehydrogenation of ethanol to CH_3CHO, dehydration to CH_2=CH_2, decomposition to CO and CH_4 or CO_2 and CH_4.

CH_3CHO and the CH_2=CH_2 are intermediary products that could be formed during reaction at relatively low temperatures before the formation of H_2 and CO_2 and it is also possible to form coke over the surface of the catalyst.

*To whom correspondence should be addressed: Email: jlcl@correo.azc.uam.mx
Phone: 53189065 ext 116, Fax: 53947378

The catalytic ethanol steam reforming has been reported to produce hydrogen and low amounts of CO and CO_2 [3-4]. Another attractive point of this reaction is related with the energy required to produce H_2. An energy balance has shown that approximately 35% of the total energy obtained by hydrogen combustion is required to produce hydrogen, whereas the remaining 65% is the available energy [5].

There are several catalysts being studied in this field. In our case, we are interested in catalysts made out of hydrotalcites. This class of catalysts has high surface area, a good basic site distribution and these solids present the so-called memory effect [6-8].

The main objective of the present research was to evaluate the effect of the addition of W (as WOx) to the production of hydrogen from ethanol steam reforming. The addition of WOx in catalysts with Al_2O_3 has resulted in a high thermal stability [9]. The second objective was to study the effect of W over the steam reforming of ethanol reaction for hydrogen production over Ni/Hydrotalcite catalysts. The authors examined the effect of W content on the conversion, selectivity and stability of the promoted catalysts. This metal is able to break C-H and C-C bonds to produce hydrogen [10-12].

NOMENCLATURE

Si (%)	Selectivity to product i
X	Conversion
Ni	Moles of product I
Nj	Moles of each product (included i)
K	Equilibrium constant
y_{CO2}	Mole fraction of CO_2
y_{H2}	Mole fraction of H_2
y_{H2O}	Mole fraction of H_2O
y_{OH}	Mole fraction of Ethanol

2. EXPERIMENTAL

2.1. Catalyst Preparation

The hydrotalcite was made by coprecipitation using two salt solutions as precursors. First, in a stirred reactor a salt solution of $Mg(NO_3)_2$ and $Al_2(NO_2)_3$ (J.T. Baker) with a molar ratio of 2:1 was made. A second solution of Na_2CO_3 (5%) and NaOH (pH = 10) (Carlo Erba) was prepared. These two solutions were added simultaneously drop by drop to a third stirred reactor using water as solvent (60 drops/min) at 60°C maintaining an atomic ratio of Mg^{2+}/Al^{3+} of 1.55. After aging the precipitate for 24 h the resulting solid was impregnated with $Ni(NO_3)_2$.

The solution of $Ni(NO_3)_2$ was added in such a way as to get a constant amount of 1 wt% Ni. The precipitate was washed, dried and calcined at 450°C for 5h. These solids were impregnated with a solution of $(NH_4)_{12}W_{12}O_{41}5H_2O$, (Aldrich) having different W concentrations: 0 wt%W and 1%Ni (sample HTN), 0.5wt%W and 1%Ni (HTN05W), 1wt%W and 1wt%Ni (HTN1W), 2wt%W and 1wt%Ni (HTN2W), 3wt%W with 1wt%Ni (HTN3W). The impregnation of the solids was made during 24 h at 60°C. The solids were washed, dried at 120°C for 24 h and calcined at 450°C during 5 h. Finally the samples were reduced with pure H_2 at 500°C for 2 h.

2.2. Catalysts Characterization

The solids obtained were characterized by X-ray diffraction (XRD) in a Phillips X´ Pert instrument. The XRD patterns of the samples after calcination were obtained using the CuKα radiation. Diffraction intensity was measured in the 2θ range between 5 and 70° with a 2θ step of 0.02° with 8 seconds per point, the samples were analyzed directly at room temperature. The infrared spectroscopy was made in a Perkin Elmer spectrophotometer (Spectrum-RX). An infrared beam was sent through a wafer of the sample. The wavenumber range was from 4000 to 400 cm^{-1} and the number of scans averaged was 50. N_2 physisorption at 77 K was made in a Micromeritics 2000 instrument. Each sample was pretreated at 200°C under vacuum (1×10^{-4} torr). The diffuse reflectance UV-visible spectroscopic analysis (UV-vis) of the samples was made in a Varian (Cary 5E) spectrophotometer. The range of wavelength was from 3000 nm to 200 nm.

2.3. Catalytic evaluation for steam reforming of ethanol

The catalytic reaction was made in a U-shaped stainless steel fixed bed reactor. The catalyst (1g) was charged for each of the reaction evaluation. The feed of the reactants consisted of ethanol (Aldrich), water as steam and N_2 (purity 99.99%, Infra-Air Products). N_2 was fed through a micrometric needle valve (1 ml/s). The gas mixture of H_2O and CH_3CH_2OH (molar ratio of 4/1) in N_2 stream was prepared using two glass saturators followed by heating to 92°C before it should be feed to the reaction chamber.

The temperature of the catalyst was changed to 450°C in flow of N_2 for 30 min to clean the catalyst surface and then the flow of reactants started at 450°C. The catalyst was held at that temperature for 30 min in order to make three analyses. In the case of deactivation tests the catalysts were evaluated during 420 min.

The analysis of the reactants and all the reaction products was carried out online by gas chromatography. Inside an automated injection valve, the sample was divided into two portions which were then analyzed in order to obtain accurate, complete quantification of the reaction products. One sample was used to analyze H_2, CO, CO_2 and CH_4, using a column of silica gel 12 grade 60/80 (18´× 1/8") with a thermal conductivity detector (Gow-Mac apparatus). The second sample was used to analyze CH_3CH_2OH, CH_3CHO, CH_3COCH_3, CH_2O and $CH_2{=}CH_2$ with a capillary column (VF-1ms, 15m × 0.25 mm) in a Varian chromatograph CP-3380 with a flame ionization detector (FID). Response factors for all products were obtained and the system was calibrated with appropriate standards before each catalytic test. The conversion (X) was calculated using the ethanol composition before and after of the reaction. The selectivity of each product was defined as follows: Si (%) = Ni / Σ Nj × 100 (see the nomenclature).

3. RESULTS AND DISCUSSION

3.1. Textural properties

The surface area (BET) and the nominal content of W are shown in Table 1. These samples were mesoporous [6] and they showed an IV type hysteresis (Figure 1) according to the IUPAC classification [13-15]. The hysteresis of the isotherms corresponded with the structure of parallel plates typical of the hydrotalcites [16]. The surface area obtained in the Ni series was nearly inversely proportional to the W concentration. This WOx effect was similar with that observed in WO_x/Al_2O_3 catalysts [9], although we did not detect surface oxo compounds by Raman spectroscopy in our samples at low W concentrations. It could be possible that WO_x species were inside the hydrotalcite structure. This possibility was strengthened by the fact that the pore volume decreased as the W concentration increased.

The sample without W (sample HTN) showed the widest pore

Table 1. Surface area BET and W concentration of the WO_x/ Ni-Hydrotalcite catalysts

Catalysts	W (% wt)	Surface area BET (m^2/g)	Pore volume by Gurvitch (cm^3/g)	Pore diameter (Å)
HTN	0	226	0.23	578
HTN05W	0.5	197	0.14	254
HTN1W	1	223	0.16	250
HTN2W	2	195	0.14	469
HTN3W	3	159	0.12	450

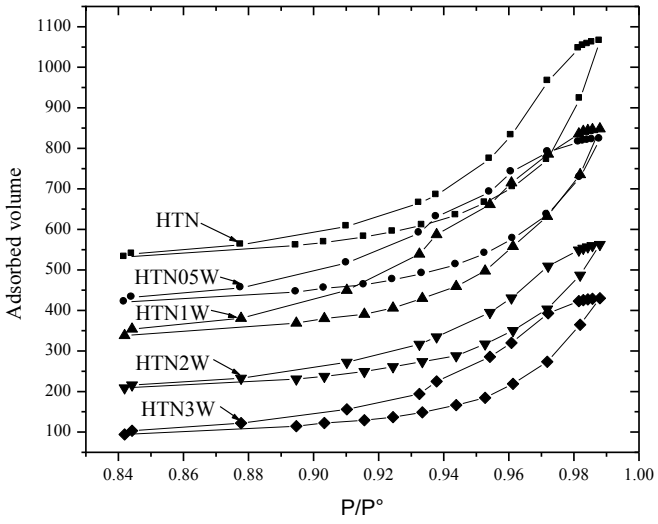

Figure 1. N_2 isotherms and the hysteresis curves for WO_x/Ni-hydrotalcite catalysts.

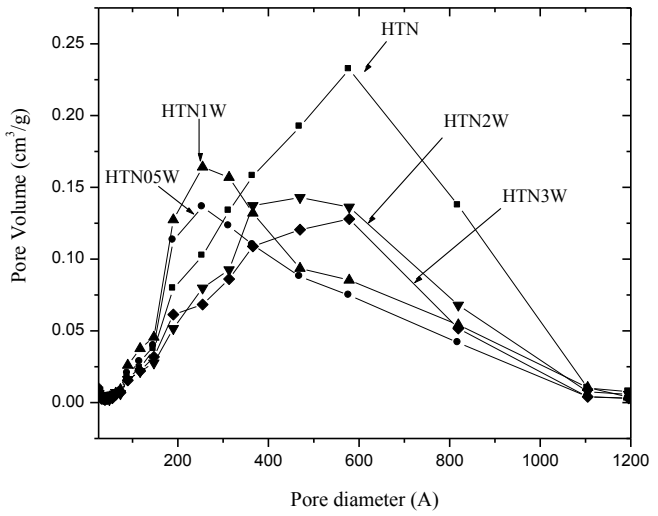

Figure 2. Pore distribution of the WOx/Ni-hydrotalcite catalysts.

distribution (50 to 1000 Å) having an average pore diameter of 578 Å (Figure 2), while the samples with the lowest W content: 0.5 and 1 wt% W (HTN05W and HTN1W) showed a smaller average pore diameter of 254 Å. In these two samples the highest effect of W occurred on the pore diameter. Indeed, these results suggest that the WO_X interacts with the hydrotalcite structure, causing a partial blockage of pores, resulting in a decrease of pores. Particularly, this phenomenon was already reported by Basile et al. [17] who suggested that such a decrease in the surface area was related to the aggregation of metallic species blocking the smaller pores and/or causing some structural rearrangements. Further addition of tungsten to the hydrotalcite (samples HTP2W and HTP3W) produced samples with pore diameter between that obtained of the HTN sample and those of the samples HTN05W and HTN1W. At small W concentrations there is pore blocking on the hydrotalcite interlay-

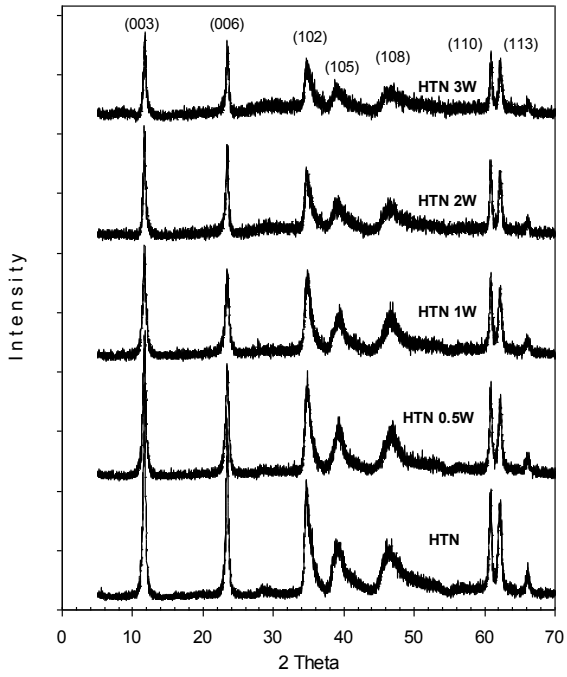

Figure 3. XRD of the WOx/Ni-hydrotalcite catalysts.

ers, thus reducing the pore diameter. While at higher concentrations of W this last one may cause the collapse of some interlayers of the hydrotalcite structure and therefore producing higher pore volumes. Another possible explanation is that at low W concentrations, W may substitute some species in the hydrotalcite structure, causing a narrower interlayer structure and therefore lower pore volumes. Further increase in W content may further incorporate more W into the hydrotalcite structure by ionic substitution that the interlayer structure may open to a pore volume comparable to the original structure without W.

3.2. XRD analysis

For samples with Ni XRD showed symmetric intense peaks corresponding to (003), (006), (110) and (113) reflections (Figure 3). Additionally, we observed asymmetric peaks with smaller intensity in (012), (015) and (018). These peaks correspond to a laminar structure typical of hydrotalcites [16]. At larger W concentration the crystalline structure of the samples decreased. The absence of other phases suggests that both W^{6+} and Al^{3+} have isomorphically replaced the Mg^{2+} cations in the burcite ($Mg(OH)_2$) - like layers [6, 10,13,18]. The intensity of the diffraction lines assigned to the hydrotalcite phase decreased by the addition of W ions, suggesting a decrease in the population of Mg-Al-Hydrotalcite structures. The Ni^{+2} and Mg^{+2} exchange could be possible [19], but that is difficult to ascertain with the low Ni concentration used.

3.3. Infrared spectroscopy

The infrared spectra for the samples with Ni are shown in Figure 4. They present a broad OH stretching band in the 3100-3700 cm^{-1} region and the H_2O scissoring mode band near 1600 cm^{-1} provides evidence for the presence of water molecules. Other authors have attributed the band at 3410 cm^{-1} to hydroxil groups coordinated

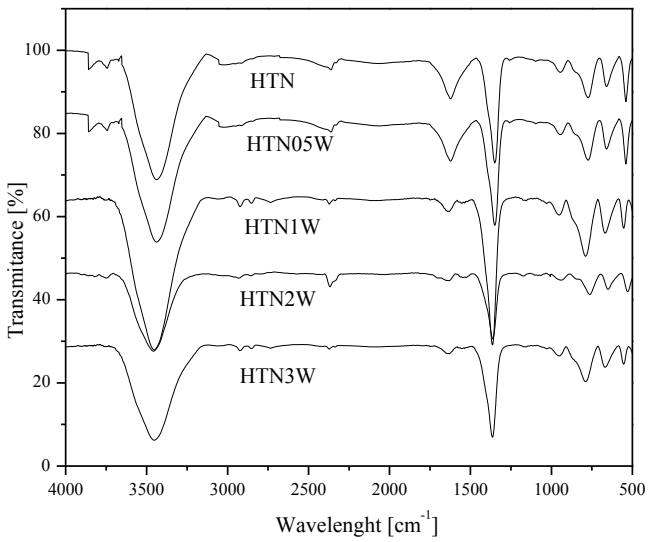

Figure 4. Infrared spectra of the WOx/Ni-hydrotalcite catalysts

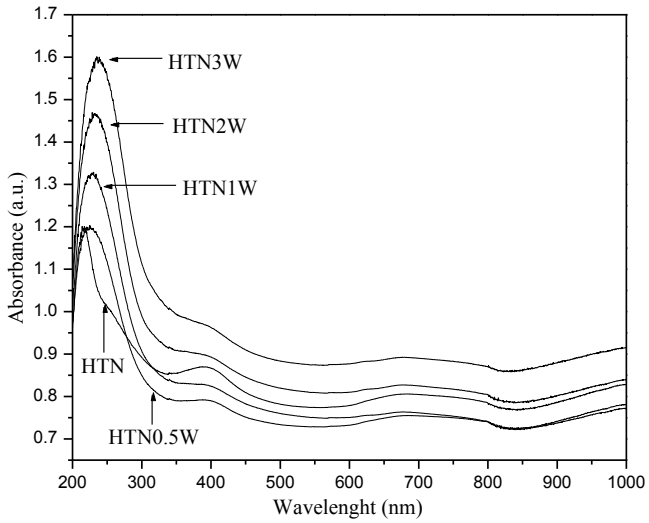

Figure 5. UV-vis spectra of the WOx/Ni-hydrotalcite catalysts

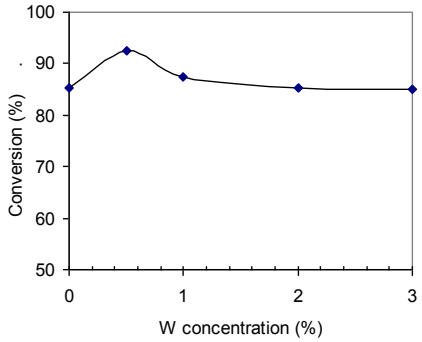

Figure 6. Effect of W concentration over the conversion for the WOx/Ni-hydrotalcite catalysts at 450°C

with Mg and Al, while the vibration of the same group associated with water is a wide band between 3650-3590 cm^{-1} [20]. The absorbance values (calculated by A = 2.3 - $\log_{10}$ % T) for this band were: 0.83, 0.73 and 0.77 for catalysts HTN2W, HTN3W and HTN 0.5W whereas 0.57 and 0.47 for catalysts HTN and HTN1W. The lowest absorbance was for the catalyst having 1 wt% W. This suggests that this catalyst had the lowest amount of hydroxil groups -OH.

A strong band located at 1380 cm^{-1} is attributed to the presence of residual nitrate ions. Another band located at 1029 cm^{-1} is related with the symmetric C=O stretching carbonate ion which has been found in 1041cm^{-1}[21]. In the region below 1000 cm^{-1} the spectrum showed a band located in 772 cm^{-1} assigned to -OH bending vibrations of brucite ($Mg(OH)_2$) type layers [22].

The bands located at 680 and 560 cm^{-1} correspond to vibration modes of brucite-type layers, specifically the metal-oxygen symmetrical stretching. The antisymmetric -OH stretching band located at 3460 cm^{-1} decreased as the W concentration increased, and so did the H_2O scissoring mode band at 1600 cm^{-1}. These results suggest that some of the –OH groups in the brucite type layers of the hydrotalcite could be substituted by WOx species.

3.4. UV-vis spectroscopy

The strong band between 200-300 nm increased as W concentration increased (Figure 5) and it has been attributed to a ligand-metal charge transfer band (LMCT) of the single ligand in W=O [22, 23]. In the case of Al_2O_3 this band increased with the W concentration, and the W^{6+} was present in a tetrahedral coordination [24-26].

It is known that the structure of the tungstate ion $[W_{12}O_{41}]^{12-}$ in aqueous solutions is highly dependent on the pH [27]. In alkaline solutions W^{6+} is present as a tetrahedral monomeric ion $[WO_4]^{2-}$. This may apply in our case, as the hydrotalcites have a basic nature.

The band between 350-450 nm is a d-d transition band assigned to the Ni-O group of NiO [28]. The band located between 650-721 nm could be ascribed to Ni^{2+} ions in octahedral coordination [28] in a $NiAl_2O_4$ -type spinel-like structure formed through diffusion of Ni ions into the support. These bands decreased as the W^{6+} ions increased, probably by substitution of Ni ions by W ions.

3.5. Catalytic activity

We observed a small promotion effect by addition of 0.5 wt % W to the Ni-hydrotalcite (Figure 6). The products of reaction were H_2, CH_3CHO, CO_2, CH_4 and $CH_2=CH_2$ (shown in Figure 7).

Ni-hydrotalcite (HTN) catalyzes ethanol steam reforming (Figures 6 and 7) as reported elsewhere [21] and the amount of Ni was not critical in the range studied. For this type of catalysts, the production of ethylene, acetaldehyde and diethyl ether vanishes at 500°C and above.

The presence of surface –OH on the catalyst has been reported to be important to catalyze the initial interaction of ethanol with these –OH groups to form ethoxy species [29] which could evolve to CH_3CHO. This compound may evolve over the surface through alkyl elimination or by forming a bidentate acetate species, which through C-C scission can produce CO_2, CH_4 and H_2 in the presence of water. This explanation may be similar for the steam reforming of ethanol using ZnO. This oxide has showed catalytic activity

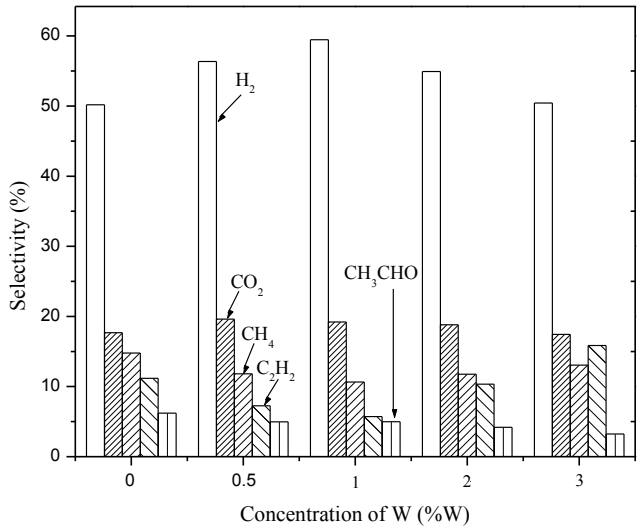

Figure 7. Reaction products from-WOx/Ni-Hidrotalcite catalysts at 450°C

producing H_2, CO_2 and CH_3CHO [29].

The reaction products in Figure 7 are produced in accordance with the following reactions:

$$CH_3CH_2OH + 3\,H_2O \rightarrow 2\,CO_2 + 6\,H_2 \quad (1)$$

$$CH_3CH_2OH \rightarrow CH_3CHO + H_2 \quad (2)$$

$$CH_3CH_2OH + H_2O \rightarrow CO_2 + CH_4 + 2\,H_2 \quad (3)$$

$$CH_3CH_2OH \rightarrow CH_2{=}CH_2 + H_2O \quad (4)$$

$$CO + H_2O \rightarrow CO_2 + H_2 \text{ (water-gas shift reaction)} \quad (5)$$

$$CH_4 + H_2O \rightarrow CO + 3\,H_2 \quad (6)$$

$$CH_2{=}CH_2 + 2\,H_2O \rightarrow CH_4 + CO_2 + 2\,H_2 \quad (7)$$

$$CH_3CHO + H_2O \rightarrow CH_4 + CO_2 + 2\,H_2 \quad (8)$$

We found CH_3CHO with all the catalysts studied, suggesting that WO_x/Ni-hydrotalcite surface acted as a dehydrogenation catalyst according to reaction (2).

Hydrogen was the main product with several reactions contributing to its production (mainly reaction 1). We did not detect CO perhaps because it reacted with water to produce CO_2 and more H_2 in accordance with reaction (5) or because reaction (1) was more favored than reactions (3) and (6) which are the route for CO production. Although some CO can be produced at thermodynamic equilibrium it may not be relevant in continuous operation because the methane reforming reaction (6) is not favored at temperatures below 450°C and it is also kinetically limited. Therefore, the most relevant reactions describing results from Figure 7 are reaction (1), (2), (3) and (4).

The ethanol dehydration to $CH_2{=}CH_2$, reaction (4) was affected by the presence of W. The catalyst with the highest W concentration showed the highest production of ethylene. In this point, the distribution of dehydration products (ethylene and diethyl ether) was dependent on both Ni and W concentrations. It has been reported [20] that for Ni-hydrotalcite catalysts, the higher the Ni loading, the lower is the selectivity to ethylene and diethyl ether. It may be possible that in our catalysts surface Ni sites could be substituted by W ions as suggested by our UV-vis spectroscopy results. If this occurred, a decrease in the concentration of Ni sites on the catalyst would favor the selectivity to the dehydration products. Additionally, it is important to remember that the presence of these products could lead to the formation of coke [30], and their yield has a space-time dependence typical of intermediate products [31].

The difference in H_2 mole fraction between all the catalysts was small and H_2 production comes from several reactions; dehydrogenation, water-gas shift conversion of CO and decomposition of oxygenated compounds. Infrared studies have shown that dehydrogenation of molecularly adsorbed ethanol was a key reaction step [32].

Ethanol adsorbs molecularly to form weakly adsorbed hydrogen-bonded species and to produce strongly adsorbed molecular ethanol on the Lewis-sites of the support. It was found that high temperature treatment of the adsorbed species caused the formation of surface acetate species on the support. The presence of water lowered the temperature for the appearance of acetate species and increased the stability of monodentate ethoxide species.

The HTN1W catalyst showed the highest production to H_2 and the lowest production to C_2H_4 (Figure 7) and moreover, it did not deactivate during 7 h on-stream (see section 3.7).

Some authors have worked with catalysts containing hydrotalcites [33] or hydrotalcite-like compound precursors with different preparation methods to produce H_2. For example, Liu et al [34] prepared their solids by a novel method, which was a combination of the reverse microemulsion and coprecipitation methods. It was observed that the precursor obtained from the above method possessed superior characteristics for preparing mixed oxide catalyst used in ethanol steam reforming. The authors mentioned that the reverse microemulsion-derived catalyst showed much better catalytic performance than catalysts prepared from conventional coprecipitation or impregnation methods in terms of H_2 selectivity and catalyst stability. However our precipitation method produced catalysts with equivalent stability during the deactivation test at 450°C. Other authors [35] prepared catalysts with Ni loaded Mg-Al mixed oxide supported catalysts which were superior in H_2 and COx product selectivity and stability compared to the pure oxide supported Ni catalysts. Recently, there are other authors using hydrotalcites or ex-hydrotalcites with other metals (La, Ce, Zn, Co, Cu) which cause a high stabilization of the active metal phases in similar way than W and with good selectivities to H_2 [36-39].

3.6. Equilibrium calculations

To get an idea of the approach to equilibrium, we performed calculations considering that reaction (1) represents the main contribution in the system [33]. Figure 8 shows the equilibrium mole fractions for the different components calculated from equation 9 using equations 10-18 to define mole fractions. We considered the 4:1 molar flow ratio of water to ethanol.

$$K = \frac{y_{CO_2}^2 y_{H_2}^6}{y_{H_2O}^3 y_{OH}} \quad (9)$$

The mole balance of the reaction (1) where X is conversion, was as

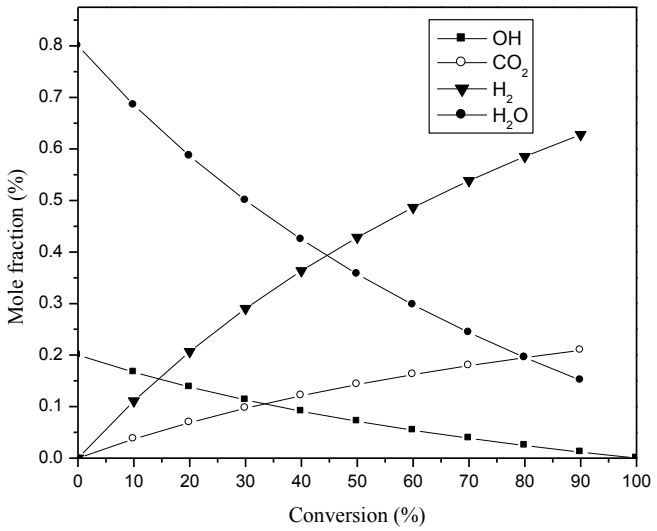

Figure 8. Mole fractions yi for each reaction product in the equilibrium calculated from Equation (9).

follows:

$$N_{OH} = (N_{OH}° - N_{OH}° X) \quad (10)$$

$$N_{CO2} = N_{OH}° 2X \quad (11)$$

$$N_{H2} = N_{OH}° 6 X \quad (12)$$

$$N_{H2O} = (N_{H2O}° - N_{OH}° 3X) \quad (13)$$

$$N = \text{Total mole flow} = N_{OH}° + 4N°_{OH}X + N_{H2O}° \quad (14)$$

The mole fractions were:

$$y_{OH} = (N_{OH}° - N_{OH}° X) / N \quad (15)$$

$$y_{CO2} = (N_{OH}° 2X) / N \quad (16)$$

$$y_{H2} = (N_{OH}° 6 X) / N \quad (17)$$

$$y_{H2O} = (N_{H2O}° - N_{OH}° 3X)/ N \quad (18)$$

The experimental and equilibrium mole fractions for H_2, CO_2, and H_2O were compared (Table 2). Only small differences were found independently of the catalyst used, suggesting that the reaction is equilibrium controlled.

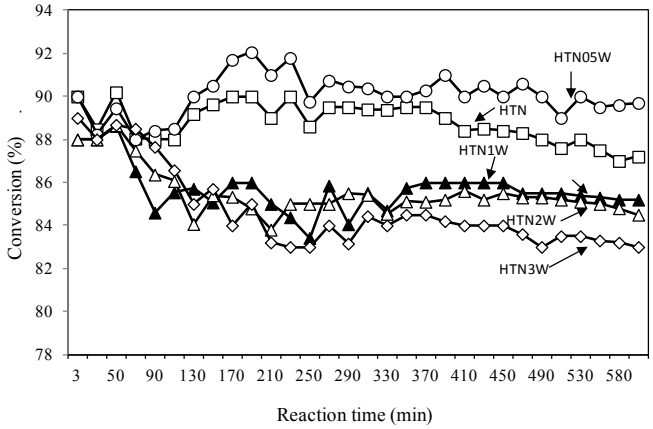

Figure 9. Long term reactions on WOx/Ni-Hydrotalcite catalysts at 450°C

3.7. Catalytic Stability

The catalysts HTN05W and HTN (0.5 and 0 wt% W) showed good stability during 420 min on-stream tests at 450°C (Figure 9). This behavior was similar to the W effect in catalysts of Pt supported on Al_2O_3 [10, 33]. In those studies, low concentrations of tungsten oxides (below monolayer, W < 1 wt %) stabilized thermally the Al_2O_3, as hydrotalcite do in this study.

4. CONCLUSIONS

The porous structure of the WOx-Ni-hydrotalcite catalysts involved parallel layers with a monomodal mesoporous distribution. It appears that Ni ions were substituted by W ions according to UV-vis spectroscopy. The surface groups determined by IR included H_2O, Al-OH, Mg-OH and CO_3^{2-}.

We observed a small promotion effect of W at low W concentrations on the Ni/hydrotalcite catalysts. The addition of 0.5 wt % W increased the selectivity to H_2 and the conversion, with the selectivity being the highest for the catalyst with 1 wt%. The catalysts studied did not produce CO and showed low selectivity to ethylene. Experimental and calculated equilibrium mole fractions of H_2 were close for the catalysts studied. The catalyst with the lowest W concentration was more stable than the catalyst without W. Catalysts with W concentrations higher than 0.5 wt% W did not show a pro-

Table 2. Experimental[1] and equilibrium mole fractions of some reaction products (considering only reaction (1)) for the WOx/Ni-hydrotalcite catalysts at 78% conversion.

Catalyst	C_2H_5OH		H_2		CO_2		H_2O	
	Exper.	Calculated	Exper.	Calculated	Exper.	Calculated	Exper.	Calculated
HT05W	0.026	0.008	0.50	0.592	0.17	0.20	0.14	0.20
HTN05W	0.033	0.008	0.56	0.592	0.19	0.20	0.15	0.20
HTN1W	0.042	0.008	0.59	0.592	0.19	0.20	0.17	0.20
HTN2W	0.051	0.008	0.54	0.592	0.18	0.20	0.17	0.20
HTN3W	0.068	0.008	0.50	0.592	0.17	0.20	0.21	0.20

[1] The experimental mole fractions of the CH_3CHO, C_2H_4 and CH_4 were not included

motion effect during long time-on-stream tests.

5. ACKNOWLEDGEMENTS

The authors acknowledge the financial support of the Universidad Autónoma Metropolitana-Azcapotzalco and UAM-Iztapalapa and the Instituto Politécnico Nacional of México.

6. REFERENCES

[1] R.D. Cortright, R.R. Davda, J.A. Dumesic, Nature, 418, 964 (2002).

[2] J. Llorca, N. Homs, J. Sales, J.L.G. Fierro and P. Ramírez de la Piscina, J. Catal., 222, 470 (2004).

[3] A. Aboudheir, A. Akande, R. Idem, A. Dalai, Int. J. of Hydrogen Energy, 31,752 (2006).

[4] Kurt Koelling, Fuel Cell Grade Hydrogen Production from the Steam Reforming of Bio-Ethanol Over Co-based catalysts: An Investigation of Reaction Networks and Active Sites. Ph.D. Thesis, The Ohio State University, (2005).

[5] M.A. Ortiz R., Hydrogen from bio-ethanol using Co, Ni and Pt hydrotalcites, stabilizated with WO_x, Chem. Eng. Thesis, UAM-Azcapotzalco, México (2009).

[6] M. de los Ángeles Ocaña Z. Síntesis de Hidrotalcitas y Materiales Derivados: Aplicaciones en Catálisis Básica. Tesis de Doctorado, Universidad Complutense de Madrid. (2005).

[7] H. Liandro Reza G., Síntesis y caracterización fisicoquímica de catalizadores sólidos básicos tipo hidrotalcita de cobalto y níquel. Tesis de licenciatura, Universidad Autónoma Metropolitana, Unidad Azcapotzalco (2003).

[8] F. Cavani, F. Trifiro, A. Vacari, Catal. Today, 11, 173 (1991).

[9] J.L .Contreras, G.A. Fuentes, J. Salmones, B. Zeifert, J. of Alloys and Compounds, 483, 371 (2008).

[10]J.L.Contreras, J. Salmones, L.A. García, A. Ponce, B. Zeifert and G.A. Fuentes, J. of New Materials for Electrochemical Systems, 11, 109 (2008).

[11]M.N. Barroso, M.F. Gómez, L.A. Arrúa, M.C. Abello, Appl. Catal. A:General, 304, 116 (2006).

[12]J. Llorca, N. Homs, J. Sales, and P. Ramírez de la Piscina, J. Catal., 209, 306 (2002).

[13]K. Sing, D. Everett, R. Haul, L. Moscou, R. Pierotti, J. Rouquerol, and T. Siemieniewska, Pure Appl. Chem. 57, 603 (1985).

[14]L. D. Gelb, K.E. Gubbins, R. Radhakrishnan, and M. Sliwinska-Bartkowiak, Reports on Progress in Physics, 62, 1573 (1999).

[15]S. Lowell, J.E. Shields, M.A. Thomas, and M. Thommes, Characterization of Porous Solid and Powders: Surface Area, Pore Size and Density, Kluwer Academic Publishers, 2004.

[16]M. del Arco, D. Carriazo, S. Gutiérrez, C. Martín and V. Rives, Inorg. Chem., 43, 375 (2004).

[17]F. Basile, G. Fornasari, M. Gazzano, A. Vaccari, Appl. Clay. Sci., 16, 185 (2000).

[18]A.C.C. Rodríguez,C.A. Enríquez, J.L.F. Monteiro, Mater. Res., 6, 563 (2003).

[19]T. Shishido, M. Sukenobu, H. Morioka, R. Furukawa, H.l Shirahase, K. Takehira, Catal. Lett., 73, 21 (2001).

[20]María de los Ángeles Ocaña Zarceño, Síntesis de Hidrotalcitas y Materiales Derivados: Aplicaciones en Catálisis Básica. Tesis de Doctorado, Universidad Complutense de Madrid (2005).

[21]C. Resini, T. Montenari, L. Barattini, G. Ramis, G. Busca, S. Presto, P. Riani, R. Marazza, M. Sisani, F. Marmottini, U. Costantino, Appl. Catal.A: General, 355, 83 (2009).

[22]A. Bartecki and D. Dembicka, J. of Inorg. and Nuclear Chem., V.29, I.12, 2907 (1967).

[23]J.L. Contreras and G.A. Fuentes, Studies in Surface Science and Catalysis, Vol. 101 Edit. B. Delmon and J.T. Yates, Elsevier 1195 (1996).

[24]A. Iannibello, L. Villa, and S. Marengo, Gazzetta Chimica Italiana, 109, 521 (1979).

[25]L. Salvati, L.E. Makovsky, J.M. Stencel, F.R. Brown, D.M. Hercules, J. Phys.Chem., 85, 3700 (1981).

[26]J.A. Horsley, I.E. Wach, JÑ. M. Brown, G.H. Via, F.D. Hardcastle, J. Phys. Chem., 91, 15, 4014 (1987).

[27]W.P. Griffith and T.D. Wickins, J. Chem. Soc. A., 1087 (1966).

[28]S. Damyanova, B. Pawelec, K. Arishtirova, J.L.G. Fierro, International Journal of Hydrogen Energy, 3610635, 10647 (2011).

[29]J. Llorca, N. Homs, P. Ramírez de la Piscina, J. of Catal., 227, 556 (2004).

[30]J.R. Rostrup-Nielsen, N. Hojlund in: J. Oudar, H. Wise (Eds.), Deactivation and Poisoning of Catalyst, Marcel Dekker, New York, Basel, p.57 (1985).

[31]J. Comas, F. Mariño, M. Laborde, N. Amadeo. Chem Eng. J. 98, 61 (2004).

[32]A. Erdohelyi, J. Rasko, T. Kecskes, M. Toth, M. Dömök, K. Baán, Catal. Today, 116, 367 (2006).

[33]J.L. Contreras, M.A. Ortiz, G.A. Fuentes, R. Luna, J. Salmones, B. Zeifert, L. Nuño and A.Vázquez, J. of New Materials for Electrochemical Systems, 13, 253 (2010).

[34]L. Liu, D. Chen, K. Zhang, J. Li, N. Shao, Int. J. of Hydrogen Energy, 33, 3736 (2008).

[35]L.J.I. Coleman, W. Epling, R.R. Hudgins, E. Croiset, Appl. Catal., A: General, 363, 52 (2009).

[36]L. He, H. Berntsen, De Chen, J. of Phys. Chem., A, Vol. 114, 3834 (2010).

[37]A.F. Lucrédio, J.D. A.Bellido, E.M. Assaf, Appl. Catal. A: General, 388, 77 (2010).

[38]G. Zeng, Q. Liu, R. Gu, L. Zhang, Y. Li, Catal. Today, 178, 206 (2011).

[39]R. Guil-López, R.M. Navarro, M.A. Peña, J.L.G. Fierro, Int. J. of Hydrogen Energy, 36, 1512 (2011).